DOI: 10.1002/cssc.201000299

Lignin Solubilization and Aqueous Phase Reforming for the Production of Aromatic Chemicals and Hydrogen

Joseph Zakzeski and Bert M. Weckhuysen*[a]

The solubilization and aqueous phase reforming of lignin, including kraft, soda, and alcell lignin along with sugarcane bagasse, at low temperatures ($T \leq 498$ K) and pressures ($P \leq 29$ bar) is reported for the first time for the production of aromatic chemicals and hydrogen. Analysis of lignin model compounds and the distribution of products obtained during the lignin aqueous phase reforming revealed that lignin was depolymerized through disruption of the abundant β–O–4 linkages and, to a lesser extent, the 5–5′ carbon-carbon linkages to form monomeric aromatic compounds. The alkyl chains contained on these monomeric compounds were readily reformed to produce hydrogen and simple aromatic platform chemicals, particularly guaiacol and syringol, with the distribution of each depending on the lignin source. The methoxy groups present on the aromatic rings were subject to hydrolysis to form methanol, which was also readily reformed to produce hydrogen and carbon dioxide. The composition of the isolated yields of monomeric aromatic compounds and overall lignin conversion based on these isolated yields varied from 10–15% depending on the lignin sample, with the balance consisting of gaseous products and residual solid material. Furthermore, we introduce the use of a high-pressure autoclave with optical windows and an autoclave with ATR-IR sentinel for on-line in situ spectroscopic monitoring of biomass conversion processes, which provides direct insight into, for example, the solubilization process and aqueous phase reforming reaction of lignin.

Introduction

With the depletion of fossil fuels as a source of fuels, chemicals, and energy, the fraction of energy and chemicals supplied by renewable resources such as biomass can be expected to increase in the foreseeable future.[1,2] One particular opportunity to produce these products arises through the catalytic valorization of lignin. Lignin is a natural amorphous three-dimensional polymer consisting of methoxylated phenylpropane structures that composes a significant portion of lignocellulosic biomass. As of 2004, the pulp and paper industry alone produced 50 million tons of extracted lignin, but only approximately 2% of the lignin available is used commercially, with the remainder used as a low-value fuel.[3] With its unique structure and chemical properties, the catalytic valorization of lignin represents a potentially useful method to obtain bulk and fine chemicals. The composition of lignin varies from plant to plant, with lignin from softwood consisting mostly of coniferyl alcohol units whereas hardwoods consist largely of syringol units, although exceptions are known.[1] The coniferyl alcohol units contain a single methoxy group while the syringol alcohol unit contains two methoxy groups. In some plant species *p*-coumaryl units, which lack methoxy groups on the aromatic ring, are found in the lignin structure. In the lignin polymer, these coniferyl, syringol, and *p*-coumaryl units are connected through various linkages.[1] The β–O–4 and 5–5′ linkages are the most abundant, constituting approximately 50–60% and 20–25%, respectively, of all linkages in lignin.[1] The remaining, less-abundant linkages present in lignin include the 4–O–5, β-β, β-5, spirodienone, dibenzodioxocin, and phenylcoumaran linkages. A schematic depiction of lignin showing these linkages is given in Figure 1.

The disruption of the linkages in lignin represents a potential route for the production of a wide range of aromatic compounds. Indeed, the depolymerization of the complicated lignin polymer into smaller platform molecules is an important aspect of lignin valorization. Previous methods to depolymerize lignin include pyrolysis, catalytic hydrogenation, oxidation, or hydrocracking.[1,4–7] US Patent Nos. 0218061A1 (2009) and 0218062A1 (2009) to Schinski et al. disclose a process for the hydrotreatment of lignin to yield aromatic products, requiring the use of a hydrogen feedstock.[8,9] Lignin treatment and gasification using supercritical water ($T_c = 647.3$ K, $P_c = 221$ bar) have also been reported to primarily form light alkanes and hydrogen,[10–17] although the disadvantages of these processes include the need for high reaction temperatures and pressures (often $T \geq 673$ K and $P \geq 250$ bar).

The aqueous-phase reforming (APR) of biomass-derived oxygenated compounds, such as methanol, glycols, glycerol, sorbitol, xylose, and glucose, has been reported for the production

[a] *Dr. J. Zakzeski, Prof. Dr. B. M. Weckhuysen*
Inorganic Chemistry and Catalysis group
Debye Institute for NanoMaterials Science
Utrecht University
Sorbonnelaan 16, 3584 CA Utrecht (The Netherlands)
Fax: (+31) 30 251 1027
E-mail: b.m.weckhuysen@uu.nl

Supporting Information for this article is available on the WWW under http://dx.doi.org/10.1002/cssc.201000299.

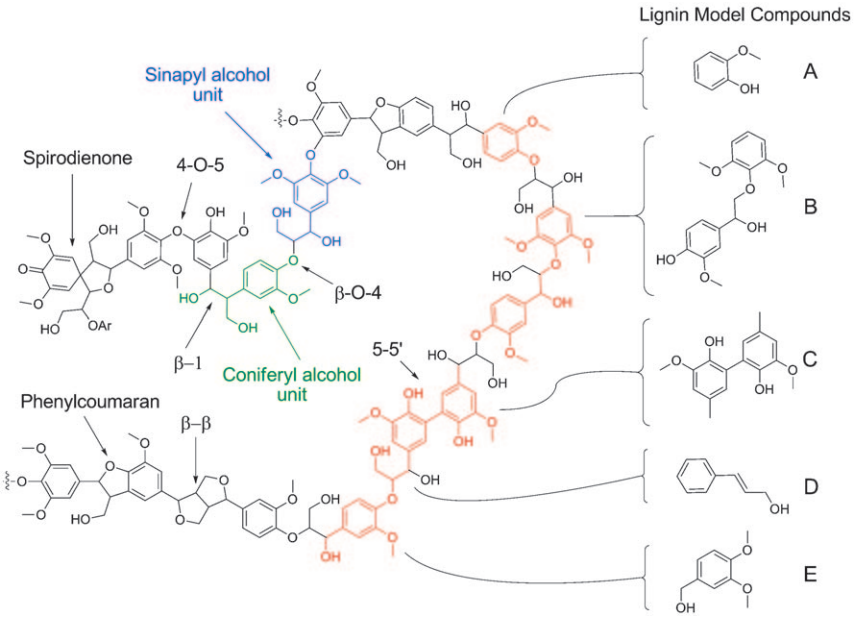

Figure 1. Schematic depiction of lignin, showing various linkages and lignin model compounds used in this study to model (A) phenol and methoxy functionality, (B) β–O–4 linkages, (C) 5–5′ linkages, (D) propyl side chain, and (E) benzylic groups. Lignin structure reproduced from Ref. [1]. Copyright 2010, American Chemical Society.

of hydrogen at temperatures ($T < 538$ K) and pressures considerably lower than those required for gasification or pyrolysis.[18] Several patents and manuscripts have been published in the field of APR of biomass-derived oxygenated compounds for the production of hydrogen and chemicals. The preferred catalysts for these systems comprise Group VIII transition metals, including alloys and mixtures, with platinum, ruthenium, or rhodium giving the most favorable results. The catalyst support is preferably selected from the group consisting of alumina, boron nitride, carbon, ceria, silica, silica-alumina, silica nitride, titania, zirconia, or mixtures thereof, with silica the preferred support.[19,20] In most reports of APR reactions, fluidized-bed tubular reactors were used, and a decrease in void-space, defined as portions of the reactor that contain no solid catalyst, resulted in higher hydrogen production.[21] In the case of actual biomass, however, the presence of solid feeds and residues increases the difficulty of developing continuous processes; thus, batch or semi-batch systems are more readily applied to the reactions.

To date, all studies of APR have focused on the use of model compounds that could be derived from biomass, such as sorbitol and glucose, and only recently the APR of actual biomass consisting of Southern pine sawdust was investigated for the production of hydrogen.[22] Only a small fraction of the lignin in the Southern pine sawdust was acid-soluble, and depolymerization occurred to a limited extent due to the formation of some acid-labile bonds, such as α- and β-ether linkages.[22]

Earlier reports of condensation caused by the acid hydrolysis of lignin is due to the intermolecular dehydration between benzylic carbon and guaiacyl aromatic rings, and sulfuric acid caused a cross-linking effect that resulted in the formation of higher molecular weight polymeric products.[22–24] Nevertheless, until this work, there have been no reports of the APR of pure lignin samples at low temperatures and pressures. The purpose of this work is therefore to demonstrate a process for the solvation and APR of lignin, exemplified with the use of soda lignin, kraft lignin, alcell lignin, and lignin from sugarcane bagasse, for the production of hydrogen and aromatic platform chemicals. Through the use of lignin model compounds and analysis of actual lignin samples, we demonstrate the capabilities of the system and the types of products obtainable by the APR of pure lignin samples. Additionally, information on these processes will be obtained with specially-designed high-pressure autoclaves equipped with optical windows and an ATR-IR sentinel providing direct in situ mechanistic insight.

Results and Discussion

Lignin solubilization in water

We began our investigation by conducting the solubilization of the lignin samples under APR conditions. As indicated above, the structural composition varies considerably from plant to plant and also depends on the pretreatment method used to obtain the lignin. The kraft lignin used in this study, for example, contains sulfur, whereas the soda lignin and sugarcane bagasse have reduced sulfur content, and the organosolv alcell lignin and is relatively sulfur-free. For the purpose of analyzing the solvation behavior of the various lignin samples used in this study, we employed a specially constructed reactor equipped with quartz windows (see Supporting Information for reactor schematic) and also a reactor equipped with a silicon sentinel for in-situ ATR-IR spectroscopy measurements.

Figure 2 depicts the visual images for the exemplary case of organosolv lignin heated from room temperature to 498 K. Initially, the organosolv lignin was insoluble in water and formed a slurry upon vigorous stirring. The color of this slurry became gradually darker as the temperature increased. The biggest change in the slurry occurred at 388 K, where a large portion of the lignin began to solubilize in the aqueous phase. Upon reaching 403 K, nearly all of the solid mass was dissolved, which resulted in a yellow-colored solution. As the temperature was increased to 498 K (the reaction temperature used for APR) the solution color turned crimson-red, possibly attributable to soluble quinones.[25] At the conclusion of the reaction,

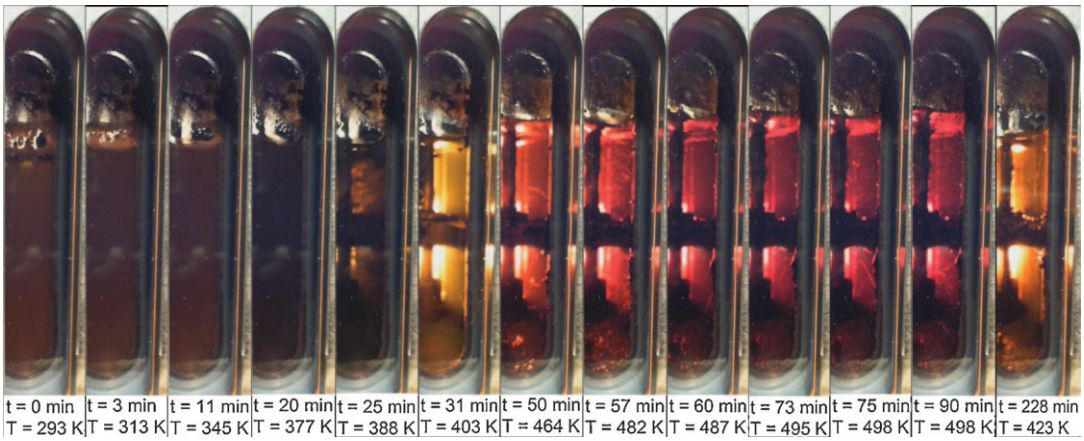

Figure 2. Visual images for the solubilization of organolv lignin in water from 298 K to 498 K, measured with the high-pressure autoclave equipped with an optical window.

the solution color reverted back to the yellow color originally observed at 403 K.

The ATR-IR spectra of the organosolv lignin dissolution are depicted in Figure 3 a, while the fingerprint regions of the spectra are given in Figure 3 b. At room temperature, the dominant vibrations observed originated from the water stretching and bending modes, and vibrations attributed to the insoluble lignin were not readily observed. The most significant change in the IR spectra occurred between 388 and 403 K, which corresponded to the appearance of several vibrations detected by ATR-IR. Two aliphatic C–H stretch vibrations were observed at 2945 and 2852 cm^{-1}, and several vibrations attributed to aromatic C–H breathing species were detected in the fingerprint region. Quinones tend to absorb strongly between 1690 and 1655 cm^{-1},[26] so the appearance of the vibration at 1695 cm^{-1} may be attributed to quinone species. The vibrations at 1508, 1460, and 1426 cm^{-1} correspond to ring carbon-carbon skeletal vibrations, which usually give three bands with the strongest near 1500 cm^{-1}.[26] The vibrations in the range 1030–1150 cm^{-1} are likely attributed to hydroxyphenyl vibrations from guaiacol and syringol groups, as supported by the appearance of similar vibrations observed in pure guaiacol samples.[26] The vibrations at 1358, 1314, and 1213 cm^{-1} may be attributed to phenolic O–H deformation and C–O stretching vibrations, which tend to appear in the ranges 1390–1330 cm^{-1} and 1260–1180 cm^{-1}.[26] The appearance of these vibrations corresponded to the formation of dissolved organic species from the lignin sample, as described above.

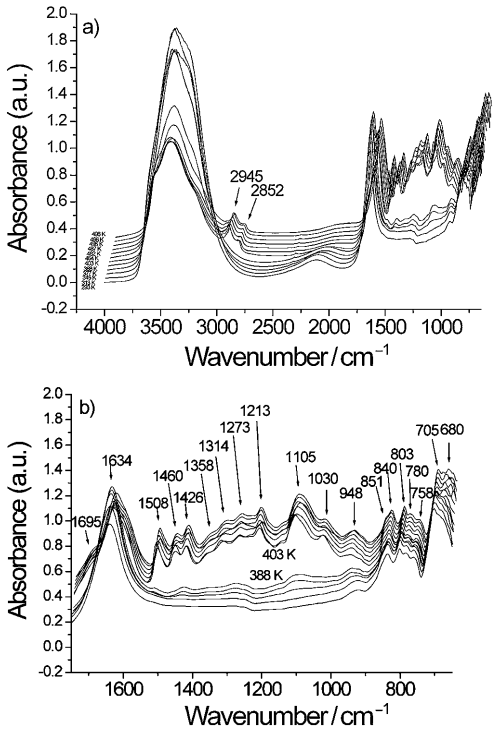

Figure 3. In situ ATR-IR spectra of the dissolution of organosolv lignin in water: a) full range spectra, and b) fingerprint region.

The behavior of the kraft lignin contrasted distinctly with the organosolv lignin. Figure 4 depicts the visual images captured during the similar treatment of kraft lignin. As with the organosolv lignin, the kraft lignin was initially water-insoluble, and a slurry formed upon vigorous stirring. In contrast to the organosolv lignin slurry, which tended to darken with increasing temperature, the kraft slurry became lighter in color as the reaction temperature was increased from 293 to 403 K. A distinct change occurred at 482 K, which corresponded to the agglomeration of solid materials in the aqueous solution. This material began to deposit near the windows at 487 K, and gas bubbles were observed to form on the solid surface at 498 K. Similarly to the organosolv lignin, the solution reverted back to a yellow color upon cooling.

The visual images and IR spectra for the other two lignin samples, namely the sugarcane bagasse and soda lignin, are given in the Supporting Information. These samples resembled the kraft and organosolv lignin in that the solution color turned red at elevated temperatures. In both cases the onset of dissolution began at 464 K. Very few solids were observed in the reactor in the case of the soda lignin, whereas black particles were readily observed in the case of the sugarcane bagasse.

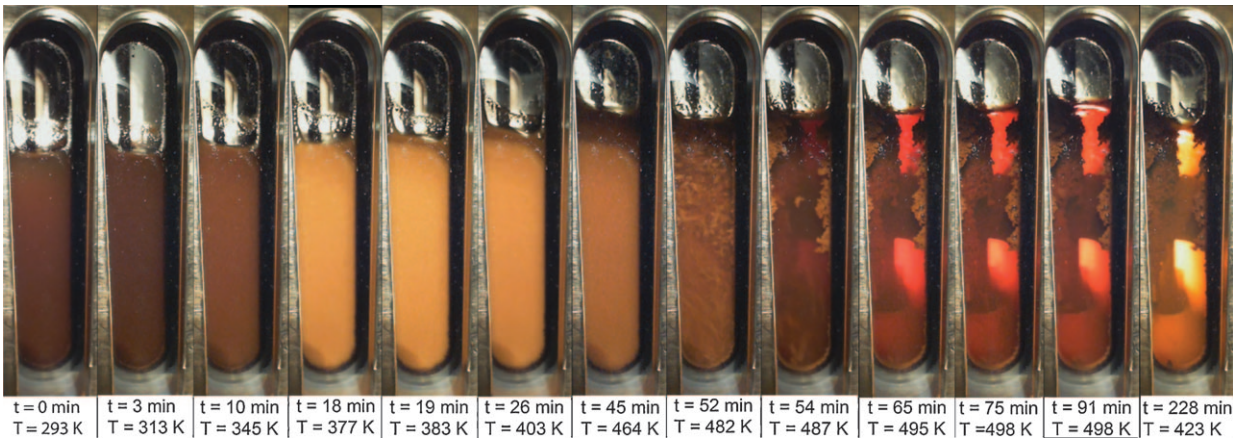

Figure 4. Visual images for the solubilization of kraft lignin in water from 298 K to 498 K, measured with the high-pressure autoclave equipped with an optical window.

The total masses of the solids recovered at the conclusion of the reaction (at 293 K) for the different lignin samples are summarized in Table 1. In accordance with the visual observations and ATR-IR spectra (Figure 5), nearly 93% of the starting organosolv lignin was solubilized with the remainder recovered as solid residue. Slightly lesser quantities were dissolved with the soda lignin, corresponding to 83% of the initial mass dissolved. As also indicated by the visual observations, solids were predominant in both the case of the sugarcane bagasse and kraft lignin, corresponding to only 51% and 38% of the initial mass dissolved, respectively. Some of the differences in solubility between the lignin samples may be attributed to the lignin particle sizes, which tended to be larger for the kraft and sugarcane bagasse lignin relative to the organosolv and soda lignin (see SEM images in the Supporting Information).

Table 1. Solids recovered during the dissolution of the various lignin samples. Reaction conditions: 200 mL H_2O, $P = 29$ bar He, $T = 498$ K, $t = 1.5$ h.

Entry	Lignin	Lignin starting mass [g]	Total recovered solid mass [g]	Pt/Al_2O_3 mass [g]	Solids from lignin [g]	Solubilized lignin [%]
1	organosolv	2.002	0.344	0.201	0.144	93
2	kraft	2.001	1.450	0.202	1.248	38
3	soda	1.998	0.548	0.200	0.348	83
4	sugarcane bagasse	1.999	1.182	0.200	0.983	51

Table 2. Solids and liquids obtained from the aqueous phase reforming of lignin samples. Reaction conditions: 10.98 g H_2O, 0.58 g H_2SO_4, 0.1245 g 1% Pt/Al_2O_3, P = 29 bar He, $T = 498$ K, $t = 1.5$ h.

Entry	Lignin	Avg. start mss [g]	Recovered solids[a] [g]	Total isolated Products [g]	GC-detected isolated products [g]	Conv. [g]
1[b]	kraft	1.384	1.302	0.026	0.012	1.9
2[c]	kraft	1.383	1.157	0.069	0.026	4.9
3	kraft	1.386	1.219	0.136	0.020	9.8
4	alcell	1.384	1.099	0.203	0.038	14.6
5	sugar-cane	1.387	0.935	0.174	0.028	12.6
6	soda	1.387	0.963	0.159	0.025	11.4

[a] After subtraction of catalyst weight. [b] No H_2SO_4. [c] No Pt/Al_2O_3.

Aqueous phase reforming of lignin

With the promising results obtained with respect to the lignin solubilization in water, we next turn our attention to the APR of the lignin samples for the production of hydrogen and aromatics. As discussed in further detail below, sulfuric acid was used in these studies, and the corrosive conditions precluded the use of the windowed reactor and in situ ATR-IR sentinel; instead, smaller, simpler autoclaves had to be used. The catalytic results of the APR of various lignin samples are given in Table 2. The columns indicate the lignin sample identity, the average starting mass of the dry lignin loaded into the autoclave, and the weight of dry solids recovered at the conclusion of the reaction not including the catalyst, which adhered to the autoclave walls and was recovered as a separate, grey-colored solid (see Supporting Information for SEM images of the solids before and after reaction). The total isolated products are the products extracted from the aqueous phase using dichloromethane and then isolated by removal of the dichloromethane solvent by rotary evaporation (see Supporting Information for NMR spectra of these isolated products). The GC-detected isolated products indicate the quantity of total isolated products detected by gas chromatography (see Supporting Information for mass spectra of materials unidentified by GC/MS). The balance between the GC detected isolated products and the total isolated products likely constitute higher molecular weight products undetectable by GC. Finally, the percent con-

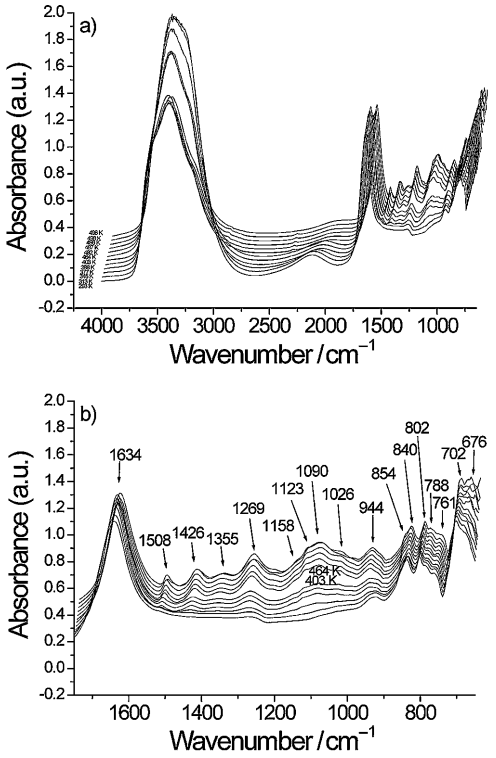

Figure 5. In situ ATR-IR spectra of the dissolution of kraft lignin in water: a) full spectra, and b) fingerprint region.

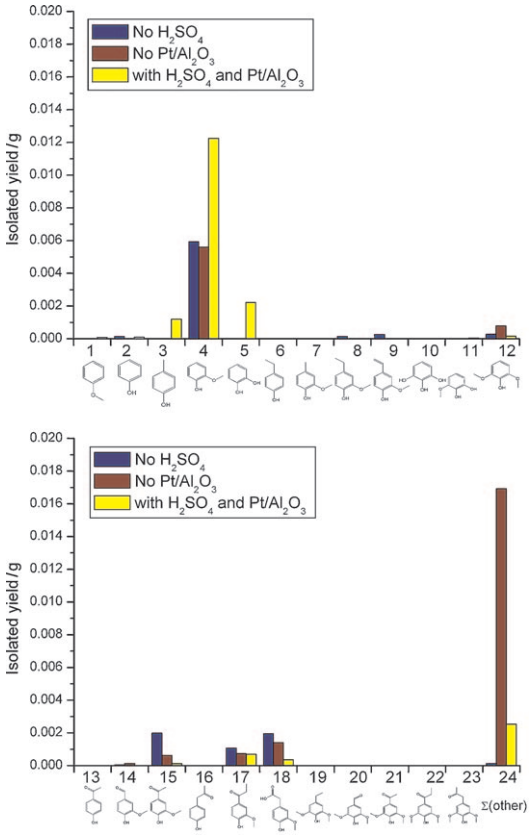

Figure 6. Composition of GC-detected isolated products from kraft lignin APR in the absence or presence of H_2SO_4 or Pt/Al_2O_3. Reaction conditions: 10.98 g H_2O, 0.58 g H_2SO_4, 1.385 g kraft lignin, 0.1245 g 1% Pt/Al_2O_3, $P = 29$ bar He, $T = 498$ K, $t = 1.5$ h.

version corresponds to the percent of lignin converted based on the recovered weight of isolated products.

Although differences exist between the lignin samples, we begin our study of the actual lignin samples using kraft lignin as an exemplary feedstock and analyze the role of the reaction components on the products obtained, particularly H_2SO_4 and Pt/Al_2O_3. The results of solids and liquids obtained from kraft lignin in the absence of H_2SO_4 are given in Table 2, entry 1. Approximately 94% of the lignin was recovered as a dark solid material, and a small number of isolated products were obtained, corresponding to 1.9% of the lignin. Discrepancies in the mass balance occur because of gas products formed and small losses attributed to solids tightly bound to the autoclave stirrer, although the latter losses are minimal. The composition of the isolated products is given in Figure 6. The other products were often complicated, high-molecular-weight compounds that were not identified by GC/MS (see Supporting Information). A majority of the isolated products consisted of coniferyl-derived products with considerably less *p*-coumaryl-, syringol-derived, and other products, as expected since the kraft lignin was obtained from pine, a softwood consisting mostly of coniferyl units. The results of kraft lignin in the presence of H_2SO_4 but in the absence of Pt/Al_2O_3, are given in Table 2, entry 2. The presence of H_2SO_4 resulted in reduced quantities of solid products recovered at the conclusion of the reaction (corresponding to 84% of the starting lignin by mass) and increased isolated yields relative to the reaction in the absence of H_2SO_4. As indicated by Figure 6, the product distribution differed considerably, with the majority of the isolated products consisting of unidentified products. Table 2 entry 3 gives the results of the APR of kraft lignin with all components present. In this case, the highest isolated yields were obtained, which corresponded to 9.8% conversion of the dry lignin to isolated products. The product distribution also varied considerably in that fewer higher-weight unidentified products were detected, which corresponded to an increase in guaiacol-derived products. These results indicate that although aromatic products are obtained in the absence of either H_2SO_4 or Pt/Al_2O_3, the highest yields of lower-molecular-weight aromatic products are obtained in the presence of both components.

As indicated by Table 2, entries 4, 5, and 6, similar results to the case of kraft lignin with all reaction components were obtained with the alcell, sugarcane bagasse, and soda lignin, in which between 73%, 68%, and 69% of the dry lignin was recovered as solids, respectively, which also corresponded to 14.6%, 12.6% and 11.4% conversion of lignin to isolated products. As shown in Figure 7, which gives the composition of the isolated products, the product distributions varied depending on the lignin samples. Whereas predominantly coniferyl-derived products were obtained from kraft lignin, including guaiacol and catechol, in the case of alcell lignin, the most abundant product observed were sinapol-derived products including syringol and the related product 1,2-diphenyl-3-me-

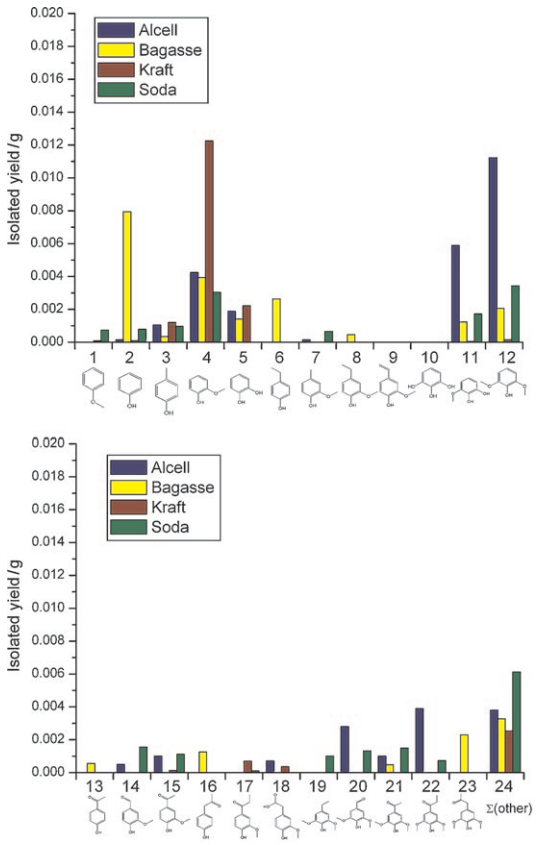

Figure 7. Composition of GC-detected isolated products from alcell, bagasse, kraft, and soda lignin APR. Reaction conditions: 10.98 g H_2O, 0.58 g H_2SO_4, 1.385 g lignin, 0.1245 g 1% Pt/Al_2O_3, $P=29$ bar He, $T=498$ K, $t=1.5$ h.

thoxybenzene followed by coniferyl-derived guaiacol. The products obtained from sugarcane bagasse, which is the residual plant material remaining after sugarcane is crushed to extract the juice, consisted predominantly of *p*-coumaryl-derived products, including phenol, although units associated with guaiacol and some syringol were also detected. Compounds with remnants of the propyl chain, such as methylphenol and ethylguaiacol were also detected, as were compounds associated with disruption of the methoxy group, such as catechol and 3-methoxycatechol. The soda lignin yielded an approximate equal mixture of coniferyl- and sinapol-derived products.

As evidenced from Table 2, a significant proportion of the original lignin was recovered as a dark brown or black solid following the APR reaction. These results contrast with the initial solubility study indicated above, in which considerably smaller quantities of material were recovered. Although this discrepancy is partially attributed to differences in reaction conditions and reactor configuration, the higher lignin starting concentrations used in the latter APR reaction also tended to result in increased solid formation relative to the lignin solubilization study.

In addition to the production of monomeric aromatic compounds indicated above, a significant characteristic of the APR of lignin involves the production of hydrogen and other useful light gases. The results of the gas phase analysis of the lignin samples at the conclusion of the reaction are given in Table 3 with the balance gas consisting mostly of the He initially charged to the autoclave. For more details of the gas composition in the autoclave at various reaction times we refer to the Supporting Information. We again begin our analysis using the exemplary case of kraft lignin and analyze the importance of the H_2SO_4 and Pt/Al_2O_3 components on the gas production. Similar results (not shown) were obtained for the other lignin samples. As indicated by Table 3, entry 1, only traces of H_2 were formed when H_2SO_4 was omitted from the system, although small quantities of lighter hydrocarbons were detected. When instead Pt/Al_2O_3 was omitted, increased quantities of H_2 were produced (Table 3, entry 2) relative to the case in which H_2SO_4 was omitted, indicating that the Pt/Al_2O_3 is not solely responsible for the production of hydrogen, an effect similarly observed during the APR of wood and other biomass.[22] The proportion of other light gases, particularly ethane, was also higher. The highest H_2 yields were obtained in the presence of both H_2SO_4 and Pt/Al_2O_3 (Table 3, entry 3). Similar results were obtained with the other lignin samples (Table 2, entries 4, 5, and 6) with the highest hydrogen yields were obtained from the alcell organosolv lignin (8.83%). In the case of all lignin samples, the hydrogen production ceased after 1.5 h of reaction (see Supporting Information).

Table 3. Autoclave gas composition following the aqueous phase reforming of the lignin samples. Reaction conditions: 10.98 g H_2O, 0.58 g H_2SO_4, 0.1245 g 1% Pt/Al_2O_3, $P=29$ bar He, $T=498$ K, $t=1.5$ h.

Entry	Lignin	H_2 [%]	CO_2 [%]	CH_4 [%]	C_2H_6 [%]	C_3H_8 [%]
1[a]	kraft	0.03	0.00	1.05	0.55	0.03
2[b]	kraft	0.47	0.00	1.10	4.36	0.00
3	kraft	4.28	0.95	2.55	3.38	0.02
4	alcell	8.83	1.52	3.06	5.52	0.06
5	sugarcane bagasse	5.03	1.14	1.98	4.26	0.03
6	soda	5.51	2.35	3.74	1.12	0.07

[a] No H_2SO_4. [b] No Pt/Al_2O_3.

Together with the analysis from the solid and liquid isolated yields, these results suggest that the H_2SO_4 aids in the disruption of the ether linkages to form monomeric aromatic compounds and hydrolysis of the methoxy groups to form methanol. The methanol and alcohol groups present on the alkyl chain of the compounds formed following the disruption of the ether linkage are then readily reformed on the Pt/Al_2O_3 catalyst to produce H_2 and other light gases. This reforming of the alkyl chain ultimately results in the formation of simpler aromatic platform molecules, such as syringol or guiacol, as reaction products. In the absence of H_2SO_4, the lignin polymer largely remains intact, which results in the decrease in both isolated product and gas yields. In the absence of Pt/Al_2O_3, the alkyl chains formed as a result of the disruption of the ether linkages by H_2SO_4 instead remain intact, resulting in reduced yields of simple molecules such as guaiacol and increased yields of compounds with more complicated alkyl chains.

As indicated above, the Pt/Al_2O_3 catalyst formed as a separate solid from the residual lignin, and it was readily isolated from the solids attributed to lignin. In order to test the recyclability and stability of the catalyst, a portion of this spent Pt/Al_2O_3 was collected at the end of the APR of organosolv lignin, dried, and immediately placed in a clean autoclave with fresh organosolv lignin. Although slightly decreased gas formation was observed, the catalyst was still highly active for the formation of hydrogen and other APR catalysts, resulting in 8.6% H_2 relative to 8.8% H_2 observed with the fresh catalyst (see Supporting Information for gas distribution versus time and SEM images of the fresh and spent catalyst). This decrease is possibly caused by small coke deposits as indicated by the darker color of the spent catalyst relative to the fresh catalyst or by pitting as a result of Al_2O_3 exposure to H_2SO_4. These results also suggest that the cessation of gas formation after 1.5 h is attributed to changes occurring to the lignin rather than deactivation of the catalyst.

Lignin model compounds

In order to elucidate the possible changes that occur to the specific linkages and functionality contained in lignin under the reaction conditions, we extend our study to the APR of several lignin model compounds. Schematic depictions of the model compounds are given in the right portion of Figure 1. The simplest model compound, guaiacol (Figure 1, species A), contains both hydroxyl and methoxy functionality, the latter of which is observed in high abundance on the aromatic constituents of lignin. Figure 8 depicts the products observed as a result of guaiacol APR under standard conditions for 90 min. In addition to unreacted guaiacol, catechol (5.8% by mass) and a small quantity of methanol were detected by GC. Similarly, along with the He initially charged to the autoclave, analysis of the gas phase at the conclusion of the reaction revealed the presence of hydrogen and carbon dioxide, which constituted 0.71% and approximately 0.12% of the total gases, respectively. These results suggest that the methoxy groups of guaiacol and, by extension and as demonstrated above, of lignin are susceptible to hydrolysis to form methanol and to produce a hydroxyl group on the aromatic ring. The methanol that forms as a result is readily reformed to form hydrogen and carbon dioxide, as previously demonstrated for pure methanol feeds.[18]

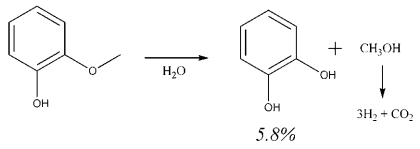

Figure 8. Aqueous phase reforming of guaiacol by a Pt/Al_2O_3 catalyst. Reaction conditions: 1.385 g guaiacol, 10.98 g H_2O, 0.58 g H_2SO_4, 0.1245 g 1% Pt/Al_2O_3, 29 bar He, 498 K, and 1.5 h.

As indicated above, the β–O–4 bond constitutes the most abundant linkage in lignin, and its disruption is thus of integral importance for the depolymerization of lignin in order to produce monomeric platform chemicals. We therefore synthesized the lignin model compound depicted in Figure 1 (species B) and subjected it to APR reaction conditions to test for possible disruption of the β–O–4 bond. The results of the reaction are given in Figure 9, where the percent yield of each product detected at the end of the reaction is indicated by the percentages below the compound.

As indicated in Figure 9, none of the starting material, the β–O–4 model compound, was detected at the conclusion of the reaction. The most abundant products detected by GC included both guaiacol (22.2% yield by mass) and syringol (22.9% yield by mass), which indicated that the β–O–4 bond was readily hydrolyzed under reaction conditions to yield monomeric products. These products were then subject to further reaction to form a variety of other products. As in the case of the pure guaiacol sample indicated above, a small portion of the methoxy groups present in the syringol and guaiacol that were formed as a result of the disruption of the β–O–4 linkage were hydrolyzed to form 1,2-dihydroxy-3-methoxybenzene (6.4%) and catechol (1.4%), respectively, along with a corresponding quantity of methanol. The balance of the β–O–4 compound was recovered as unidentified products and solid residue (138 mg–125 mg catalyst = 13 mg solids), which likely formed via a repolymerization of the components following disruption of the β–O–4 bond. In addition, small quantities of ethyl- and methyl-guaiacol possibly formed as a result of hydrogenation of the alcohol group on the alkane chain. H_2 (7.50%) and CO_2 (0.20%) along with small quantities of methane and ethane (<1%) were produced during the course of the reaction. The production of these gases greatly exceeded the case of pure guaiacol (see above), from which H_2 is formed solely through hydrolysis of the methoxy group and subsequent reforming of methanol. These results, and the high abundance of guaiacol (formed from the β–O–4 compound) suggest that the alcohol-containing alkyl chains of the latter products are highly susceptible to APR to form H_2, CO_2, and guaiacol. This catalytic reforming also occurs at a higher rate than does the hydrolysis of the methoxy groups as evident by the higher abundance of guaiacol and syringol relative to catechol and 1,2-dihydroxy-3-methoxybenzene, respectively.

The appearance of guaiacol formed as a result of the reforming of the alkyl chain of the β–O–4 model compound provided an indication for the disruption of carbon-carbon bonds during the APR reaction. As indicated above, a carbon-carbon bond, in the form of the 5–5′ linkage in lignin, is the second-most abundant linkage in lignin, and its disruption is therefore also important for the formation of monomeric aromatic compounds. In order to test the susceptibility of 5–5′ linkages in lignin to disruption, the model compound depicted in Figure 1 species C was synthesized and subjected to APR. The results are depicted in Figure 10, with the relative yield percentages by mass given below the compounds. Analysis of the solution at the conclusion of the reaction revealed the presence of methylguaiacol (7%) and guaiacol (14%), which indicated that the 5–5′ bond was susceptible to disruption under the APR conditions. This result is significant because the 5–5′ bond is

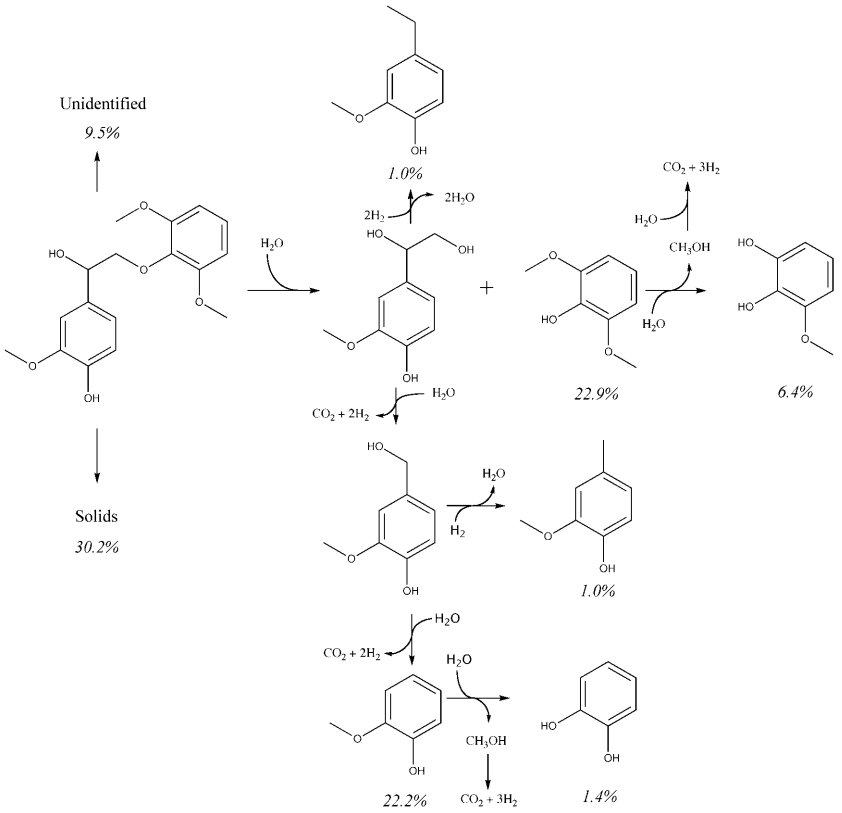

Figure 9. Products obtained during the aqueous phase reforming of the β–O–4 model compound by a Pt/Al_2O_3 catalyst. Reaction conditions: 0.043 g β–O–4 compound, 10.98 g H_2O, 0.58 g H_2SO_4, 0.1245 g 1% Pt/Al_2O_3, 29 bar He, 498 K, and 1.5 h.

very difficult to break. In contrast to the β–O–4 model compound, a small proportion of unreacted starting material (16%) was recovered at the conclusion of the reaction along with some heavy, unidentified products (estimated at 14% of the starting material). The most abundant compound, however, was obtained as a result of the hydrolysis of one or both of the methoxy-groups (in 42% and 9% yield, respectively) of the 5–5′ compound to form methanol.

In contrast to the model compounds discussed above, in which the ether bonds were decomposed to form methanol or monomeric compounds, the reaction products obtained from both cinnamyl alcohol and veratryl alcohol (Figure 1, species D and E, respectively) displayed evidence of coupling reactions. In the case of veratryl alcohol, less than 1% of the original veratryl alcohol was recovered as monomeric reaction products, such as guaiacol, 1,2-dimethoxyphenol, and catechol. Instead, the remainder of the material formed a black, solid material, which, as discussed below, resembled in appearance the solid material collected at the conclusion of the reaction of the different lignin compounds. No solids were formed when cinnamyl alcohol was used as a substrate. Instead, a large oily substance was recovered. GC/MS analysis indicated the presence of several diaryl isomers coupled by propyl chains completely devoid of oxygen-containing functionality. Since cinnamyl alcohol only contains a single alcohol group that was consumed during the course of the reaction, the reaction stopped at these dimeric products rather than the polymeric products obtained with veratryl alcohol. A large quantity of H_2 and CO_2 (8.03% and 0.12%, respectively) was obtained relative to either guaiacol (0.71% H_2 and 0.12% CO_2) or veratryl alcohol (1.89% H_2 and 0.11% CO_2), which again suggests that the reforming of the side chain in lignin occurs at a faster rate than does the hydrolysis of the methoxy groups and subsequent reforming of the resulting methanol. In addition, the high reactivity of these model compounds to form polymeric compounds in the case of

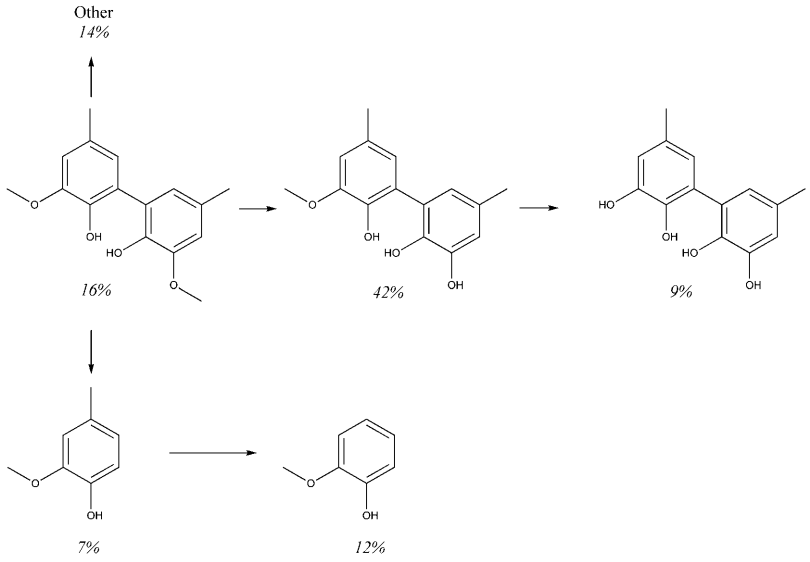

Figure 10. Products obtained during the aqueous phase reforming of the 5–5′ model compound by a Pt/Al_2O_3 catalyst. Reaction conditions: 0.042 g 5–5′ compound, 10.98 g H_2O, 0.58 g H_2SO_4, 0.1245 g 1% Pt/Al_2O_3, 29 bar He, 498 K, and 1.5 h.

veratryl alcohol and dimeric compounds in the case of cinnamyl alcohol also provides insight regarding the formation of the black solids obtained during the lignin APR.

Taken together, the results of the APR of the lignin model compounds revealed several possible reactions expected to occur with actual lignin samples. The first is that the most important linkages in lignin, the β–O–4 and 5–5′, are susceptible to disruption, although disruption of the former occurs much more readily than the latter. These disruptions are key steps necessary for the production of monomeric compounds. Following the disruption of the β–O–4 ether linkage, the alcohol-containing alkyl side chain is readily reformed to produce H_2 and CO_2, suggesting the possibility of obtaining guaiacol and syringol platform chemicals from lignin. The methoxy groups present in the model compounds were also susceptible to hydrolysis to form methanol, which was readily reformed. Even in the case of the simple model compounds, however, recondensation reactions occurred to yield high molecular weight products and other solids.

Conclusions

The solubilization and APR reaction of pure lignin samples, including soda, kraft, alcell, and sugarcane bagasse, represents a possible method to obtain hydrogen, light gases, and aromatic platform molecules, such as guaiacol, syringol and other similar products. The resulting aromatic products are readily separated from the aqueous phase by extraction. Analysis of lignin model compounds suggests that the most abundant linkages in lignin, the β–O–4 ether and, to a lesser extent, the 5–5′ carbon-carbon linkages, are disrupted under the reaction conditions to form monomeric aromatic compounds. Hydrolysis of the methoxy functionality on the aromatic rings leads to the formation of methanol, which is readily reformed to produce hydrogen and carbon dioxide. The highest yields of products were obtained in the presence of both H_2SO_4 and Pt/Al_2O_3, although products were still obtained in the absence of either component. The aromatic product distribution, in terms of the number of methoxy group present on the isolated compounds, depended on the lignin source.

Experimental Section

Soda lignin (56.15% C, 6.06% H, 0.79% N, 3.77% S) was obtained from sisal pulping black liquor, which was acidified with sulphuric acid to pH 1, filtered through laboratory paper, and dried for 2 h at 328 K. The alcell lignin (66.47% C, 5.96% H, 0.15% N, 27.43% O by difference) was isolated by the Organosolv extraction method. The INDULIN AT kraft lignin (63.25% C, 6.05% H, 0.94% N, 1.64% S, 28.12% O by difference) was obtained from pine and is free from all hemicellulosic materials. The lignin from sugarcane bagasse (58.90% C, 4.90% H, 0.14% N, 1.53% S, 34.53% O by difference) was derived from Brazilian sugarcane (see the work of Frollini et al. for additional characterization information regarding this substrate[27,28]). SEM images of the lignin samples before reaction and the solid residues collected after reaction are given in the Supporting Information.

The lignin solubilization studies were conducted in a semi-batch 200 mL autoclave equipped with quartz windows, thermocouple, pressure gauge and transducer, magnetic driver (750 rpm), and back-pressure regulator set at 29 bar. Details of this set-up can be found in the Supporting Information. Lignin samples were stored in a desiccator prior to use. During a typical treatment, 2.000 g lignin (either kraft, alcell, sugarcane bagasse, or soda) was added to the autoclave with 0.200 g Pt/Al_2O_3 (1% Pt) and 200 mL H_2O. The autoclave was then sealed, purged and charged with 29 bar He, and finally heated at approximately 4 K min^{-1} to 498 K. In situ ATR-IR measurements were recorded using a silicon sentinel equipped at the bottom of the autoclave.

The aqueous phase reforming reactions were conducted in a semi-batch 40 mL autoclave equipped with thermocouple, pressure transducer and gauge, magnetic driver (750 rpm), and back-pressure regulator set at 29 bar. Lignin samples were stored in a desiccator prior to use. During a typical reaction, lignin (either kraft, alcell, sugarcane bagasse, or soda) was added to the autoclave along with 0.125 g Pt/Al_2O_3 (1% Pt), 10.98 g H_2O, and 0.58 g H_2SO_4. The autoclave was then sealed, purged with He, and then 29 bar He was charged to the autoclave. The autoclave was then rapidly heated to 498 K in the course of about 15 min. Gas sampling was conducted using a dual-column Galaxie micro gas chromatography unit. After the designated time (typically 1.5 h), the autoclave was cooled in an ice water bath and vented.

At the conclusion of the reaction, the liquid phase was separated from solids, and finely dispersed solids were isolated by centrifugation if necessary. Products contained in the liquid phase were isolated by three sequential extractions using approximately 9 g dichloromethane, and isolated yields were obtained by removal of the dichloromethane solvent using a rotary evaporator at 310 K. The extracted products, which were often of a yellow, oily consistency, were weighed and dissolved in ethyl acetate. Chemical composition of the isolated yields was determined by Varian GC equipped with a VF-WAXms capillary column equipped with an FID detector. Hexadecane was used as an internal standard. The quantity of unknown products was estimated using the response factor determined for vanillyl alcohol. Product identification was conducted using a Shimadzu GCMS-QP2010 equipped with a VF-WAXms capillary column and by comparison with pure compounds when available.

Solids, both residual lignin and the catalyst, were often bound to the stirrer or the autoclave wall. These materials were meticulously collected from the autoclave, washed with water, and dried in an oven at 393 K overnight before weighing.

NMR measurements were conducted using Varian 400 MHz or Varian 600 MHz spectrometers. The isolated solid lignin was dissolved in deuterated DMSO, which was used as the lock source. Scanning electron micrographs were measured using a Panalytical Phenom SEM in back scatter mode.

The β–O–4 model compound was synthesized as previously described.[29] During the reaction of the lignin model compounds, 1.385 g of substrate was used instead of lignin samples except in the case of the β–O–4 and 5–5′ model compounds, in which cases 0.042 g of the substrates were used.

Acknowledgements

The authors thank the National Science Foundation International Research Fellowship Program for support of this research under Award No. 0856754, and Wouter Huijgen and Jaap van Hall (ECN), Richard Gosselink (Wageningen University), and Matthijs

Ruitenbeek and Rui Cruz (The Dow Chemical Company) for kindly supplying the lignin samples. We also thank Pieter C. A. Bruijnincx, Anna L. Jongerius, Ilona van Zandvoort, and Dilek Boga (Utrecht University) for many useful discussions, model compounds synthesis, scanning electron micrograph acquisition, and assistance with the APR equipment, respectively.

Keywords: aqueous phase reforming · aromatics · catalysis · hydrogen · lignin

[1] J. Zakzeski, P. C. A. Bruijnincx, A. L. Jongerius, B. M. Weckhuysen, *Chem. Rev.* **2010**, *110*, 3552 – 3599.
[2] F. G. Calvo-Flores, J. A. Dobado, *ChemSusChem* **2010**, *11*, 1227 – 1235.
[3] R. J. A. Gosselink, E. de Jong, B. Guran, A. Abächerli, *Ind. Crops Prod.* **2004**, *20*, 121 – 129.
[4] E. Dorrestijn, L. J. J. Laarhoven, I. W. C. E. Arends, P. Mulder, *J. Anal. Appl. Pyrolysis* **2000**, *54*, 153 – 192.
[5] P. F. Britt, A. C. Buchanan, M. J. Cooney, D. R. Martineau, *J. Org. Chem.* **2000**, *65*, 1376 – 1389.
[6] M. Misson, R. Haron, M. F. A. Kamaroddin, N. A. S. Amin, *Bioresour. Technol.* **2009**, *100*, 2867 – 2873.
[7] R. W. Thring, J. Breau, *Fuel* **1996**, *75*, 795 – 800.
[8] W. L. Schinski, A. E. Kuperman, J. Han, D. G. Naae, *Process for Generating a Hydrocarbon Feedstock from Lignin*, US 2009/0218062A0218061, **2009**.
[9] W. L. Schinski, A. E. Kuperman, J. Han, D. G. Naae, *Process for Generating a Hydrocarbon Feedstock from Lignin*, US 2009/0218061A0218061, **2009**.
[10] K. Ehara, D. Takada, S. Saka, *J. Wood Sci.* **2005**, *51*, 256 – 261.
[11] M. Saisu, T. Sato, M. Watanabe, T. Adschiri, K. Arai, *Energy Fuels* **2003**, *17*, 922 – 928.
[12] M. Osada, T. Sato, M. Watanabe, T. Adschiri, K. Arai, *Energy Fuels* **2004**, *18*, 327 – 333.
[13] T. Furusawa, T. Sato, M. Saito, Y. Ishiyama, M. Sato, N. Itoh, N. Suzuki, *Appl. Catal. A* **2007**, *327*, 300 – 310.
[14] M. Osada, N. Hiyoshi, O. Sato, K. Arai, M. Shirai, *Energy Fuels* **2007**, *21*, 1854 – 1858.
[15] M. Osada, N. Hiyoshi, O. Sato, K. Arai, M. Shirai, *Energy Fuels* **2007**, *21*, 1400 – 1405.
[16] M. Osada, O. Sato, K. Arai, M. Shirai, *Energy Fuels* **2006**, *20*, 2337 – 2343.
[17] T. Sato, T. Furusawa, Y. Ishiyama, H. Sugito, Y. Miura, M. Sato, N. Suzuki, N. Itoh, *Ind. Eng. Chem. Res.* **2006**, *45*, 615 – 622.
[18] R. D. Cortright, R. R. Davda, J. A. Dumesic, *Nature* **2002**, *418*, 964.
[19] R. D. Cortright, J. A. Dumesic, *Low-Temperature Hydrogen Production from Oxygenated Hydrocarbons*, US 6.699.457 B692, **2004**.
[20] R. D. Cortright, J. A. Dumesic, *Low-Temperature Hydrogen Production from Oxygenated Hydrocarbons*, US 6.964.758 B962, **2005**.
[21] G. W. Huber, R. D. Cortright, J. A. Dumesic, *Angew. Chem.* **2004**, *116*, 1575 – 1577; *Angew. Chem. Int. Ed.* **2004**, *43*, 1549 – 1551.
[22] M. B. Valenzuela, C. W. Jones, P. K. Agrawal, *Energy Fuels* **2006**, *20*, 1744 – 1752.
[23] I. Hasegawa, Y. Fujii, K. Yamada, C. Kariya, T. Takayama, *J. Appl. Polym. Sci. Appl. Polym. Sci.* **1999**, *73*, 1321 – 1328.
[24] Y. Matsushita, S. Yasuda, *Bioresour. Technol.* **2005**, *96*, 465 – 470.
[25] C. Heitner, D. R. Dimmel, J. A. Schmidt, *Lignin and Lignans: Advances in Chemistry*, CRC Press, Boca Raton, **2010**.
[26] G. Socrates, *Infrared and Raman Characteristic Group Frequencies: Tables and Charts*, Wiley, New York, **2001**.
[27] J. L. Guimarães, E. Frollini, C. G. da Silva, F. Wypych, K. G. Satyanarayana, *Ind. Crops Prod.* **2009**, *30*, 407 – 415.
[28] W. Hoareau, F. B. Oliveira, S. Grelier, B. Siegmund, E. Frollini, A. Castellan, *Macromol. Mater. Eng.* **2006**, *291*, 829 – 839.
[29] J. Zakzeski, A. L. Jongerius, B. M. Weckhuysen, *Green Chem.* **2010**, *12*, 1225 – 1236.

Received: September 13, 2010
Revised: October 28, 2010
Published online on January 18, 2011

